Behavior of Cement-Treated Soils in Flexure

LUTFI RAAD

Response and fracture of cement-treated layers in flexure are significantly influenced by their load-deformation characteristics in tension and compression and their tensile strength. The purpose of this paper is to use the flexure beam test to investigate the flexural behavior of a cement-treated silty clay and a cement-treated sand mix. Specifically, material properties such as tensile and compressive moduli, flexural moduli, tensile strength, flexural strength, and tensile strain at failure are determined for different compaction variables, cement contents, and curing ages. The observed difference in tensile and compressive moduli (i.e., bimodular properties) is explained using proposed mechanistic models, and the practical significance of bimodular behavior is illustrated.

Cement-treated subbases and bases in pavement structures are subjected to flexural stresses and strains under applied traffic loads. Response prediction and fracture behavior of these layers are significantly influenced by tensile strength and tensile and compressive stress-strain properties (*1, 2*). Although these properties can be determined by direct tension and compression testing, the flexural test is believed to simulate better the mode of stress to which a road base is subjected by wheel loading. The flexural modulus and flexural strength are determined in this case by using simple beam-theory assumptions (*3–5*). Strength and modulus values determined, however, do not account for possible nonlinear stress-strain behavior and different stress-strain properties in tension and compression.

The purpose of this paper is to illustrate the use of the flexure test to predict the load-deformation behavior of stabilized soils in tension and compression. Flexural beam tests are conducted on a cement-treated silty clay and a cement-treated sand mix compacted at different densities and moisture contents. Material properties such as tensile and compressive moduli, flexural moduli, tensile strength, flexural strength, and tensile strain at failure are determined for different compaction variables, curing age, and cement content. The difference of stress-strain properties in tension and compression (i.e., bimodular properties) is explained by using proposed mechanistic models, and the practical significance of bimodular behavior in response prediction and fracture of stabilized layers is illustrated.

American University of Beirut, 850 Third Avenue, New York, N.Y. 10022. Current affiliation: Department of Civil Engineering, University of Alaska, 306 Tanana Drive, Fairbanks, Alaska 99775.

EXPERIMENTAL INVESTIGATION

Flexural beam tests were conducted on compacted specimens of a cement-treated silty clay and a cement-treated sand mix. The properties of the silty clay and the sand mix are summarized in Table 1. Test group, level of treatment, curing age, and compaction data are summarized in Tables 2 and 3. Beam specimens 21 × 6 × 6 in. were prepared by using a drop hammer compactor (10 lb, 18-in. drop height). Each specimen was compacted in seven layers, and the number of blows per layer was determined for four energy levels that varied from 100 to 26 percent modified AASHTO compaction energy. The compaction curve associated with a given energy was defined by using a five-point representation in terms of dry density and compaction moisture content. After compaction, the specimens were wrapped in polyethylene sheets and cured in a humid room at 73°F. At the end of the curing period, specimens were air dried in the laboratory for 1 week, after which 1-in.-long SR-4 strain gauges were glued to the top and bottom of the beam specimens in the middle third portion. The load was applied through a loading head at a constant rate of displacement equal to 0.0120 in./min. Vertical deflections at the center of the beam specimens were measured by using a 0.00010-in. dial gauge. The applied load, strains, and vertical deflections were monitored continuously during testing. A schematic representation of the testing apparatus is shown in Figure 1.

RESULTS

The stress-strain behavior was determined with simple beam theory for a given applied load but with the assumption that the tensile and compressive moduli for the same load were different. In this case, the compressive stress σ_c and tensile stress σ_t at the top and bottom of the beam are given by

$$\sigma_c = \frac{3M}{bh^2} \frac{(\varepsilon_c + \varepsilon_t)}{\varepsilon_c} \tag{1}$$

$$\sigma_t = \frac{3M}{bh^2} \frac{(\varepsilon_c + \varepsilon_t)}{\varepsilon_t} \tag{2}$$

TABLE 1 GRADATION, SPECIFIC GRAVITY, AND INDEX PROPERTIES OF SOILS

	Silty Clay	Sand Mix
No. 4–No. 10 (%)	2	–
No. 10–No. 40 (%)	3	12
No. 40–No. 200 (%)	10	73
Percent less than No. 200	85	15
Percent less than 2μ	20	2
Specific gravity	2.71	2.67
Liquid limit	27	NP
Plasticity index	13	NP
AASHTO classification	A-6	A-2-4
Unified classification	CL	SM

NOTE: Sand mix is composed of a mixture of medium uniform sand and silty clay in a 5:1 ratio by weight.

where

ε_c = measured compressive top strain,
ε_t = measured tensile bottom strain,
M = moment at central section of beam,
b = width of beam, and
h = depth of beam.

The corresponding compressive modulus E_c and tensile modulus E_t for the same applied load could be determined as follows:

$$E_c = \frac{3M}{bd^2} \frac{(\varepsilon_c + \varepsilon_t)}{\varepsilon_c^2} \tag{3}$$

$$E_t = \frac{3M}{bd^2} \frac{(\varepsilon_c + \varepsilon_t)}{\varepsilon_t^2} \tag{4}$$

and the bimodular ratio (E_c/E_t) is expressed as

$$E_c/E_t = (\varepsilon_t/\varepsilon_c)^2 \tag{5}$$

Flexural moduli values $\overline{E}_f$ and E_f based on moment curvature equations and deflection at the center of the beam, respectively, were also determined by using the following relations:

$$\overline{E}_f = \frac{PL}{3I}\left(\frac{h}{\varepsilon_c + \varepsilon_t}\right) \tag{6}$$

$$E_f = \frac{23}{648}\left(\frac{PL^3}{dI}\right) \tag{7}$$

where

P = applied load at third points,
L = length of beam,
I = moment of inertia of beam cross section, and
d = deflection at center of beam.

Values of $\overline{E}_f$ and E_f have been used by many investigators (*3, 6, 7*) to characterize stabilized materials in flexure. These values, however, are determined by using simple beam-theory assumptions without accounting for the bimodular behavior of the material.

Flexural beam test results of cement-treated silty clay and cement-treated sand mix are presented below. All modulus values, unless otherwise specified, are determined by using the initial tangent to the load-deflection, load-tensile strain, and load-compressive strain relations.

TABLE 2 COMPACTION DATA FOR CEMENT-TREATED SILTY CLAY

Test Group	Cement Content (%)	Curing Age (days)	Compaction Energy (blows/layer)[a]	Compaction Moisture Content (%)	Maximum Dry Density (lb/ft^3)	Optimum Moisture Content (%)
C_1	11	42	240	Variable	132.0	10.44
C_2	11	42	170	Variable	130.9	11.12
C_3	11	42	107	Variable	129.5	11.49
C_4	11	42	64	Variable	125.9	12.15
C_5	3,5,7,9,11	42	240	9.96	—	—
C_6	11	1,7,14,42	240	11.66	129.3	—

[a]Seven layers.

TABLE 3 COMPACTION DATA FOR CEMENT-TREATED SAND MIX

Test Group	Cement Content (%)	Curing Age (days)	Compaction Energy (blows/layer)[a]	Compaction Moisture Content (%)	Maximum Dry Density (lb/ft^3)	Optimum Moisture Content (%)
S_1	9	42	240	Variable	127.6	9.20
S_2	9	42	170	Variable	122.6	10.65
S_3	9	42	107	Variable	122.0	10.90
S_4	9	42	64	Variable	118.8	11.72
S_5	3,5,7,9,11	42	240	9.25	—	—
S_6	9	1,7,14,42	240	9.31	120.4	—

[a]Seven layers.

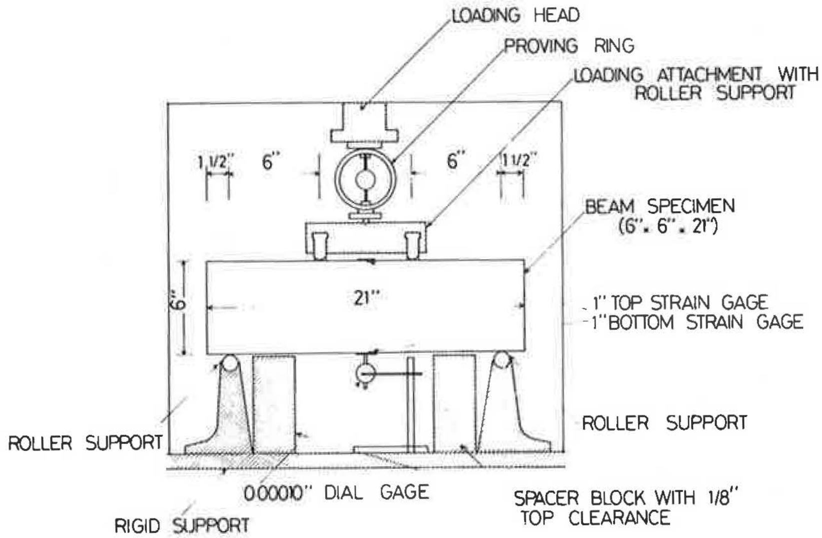

FIGURE 1 Flexural beam test apparatus.

These values are for test groups C_1–C_6 and S_1–S_6 with compaction variables summarized in Tables 2 and 3.

1. The stress-strain relationships for the cement-treated silty clay (Figure 2) and the cement-treated sand mix (Figure 3) determined by using Equations 1 and 2 are nonlinear and exhibit different behavior in compression and in tension in that the compressive modulus is larger than the tensile modulus for a given applied stress.

2. The variation of tensile strength, tensile strain at failure, and tensile, compressive, and flexural moduli with compaction moisture content by using modified AASHTO compaction energy is shown in Figures 4 and 5. The moduli in tension and compression are different, and the bimod-

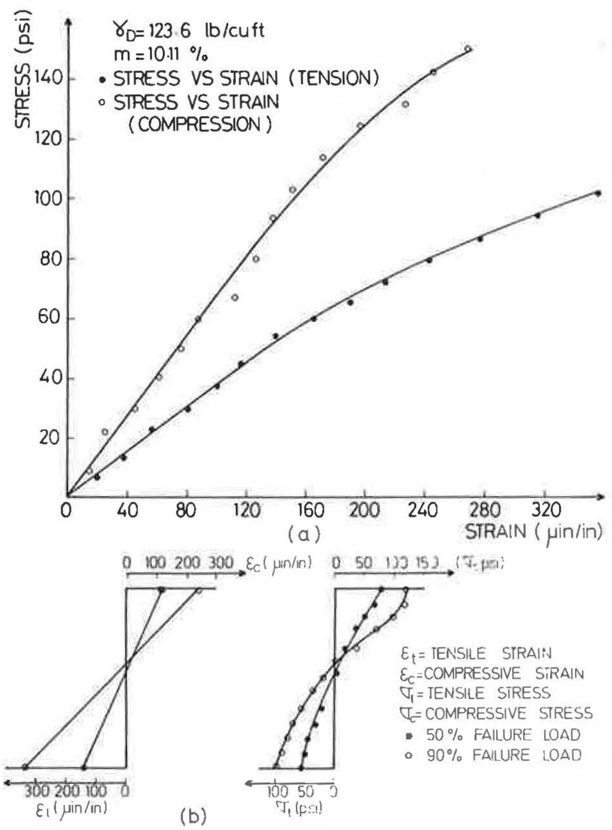

FIGURE 2 Stress-strain behavior of cement-treated silty clay in tension and compression.

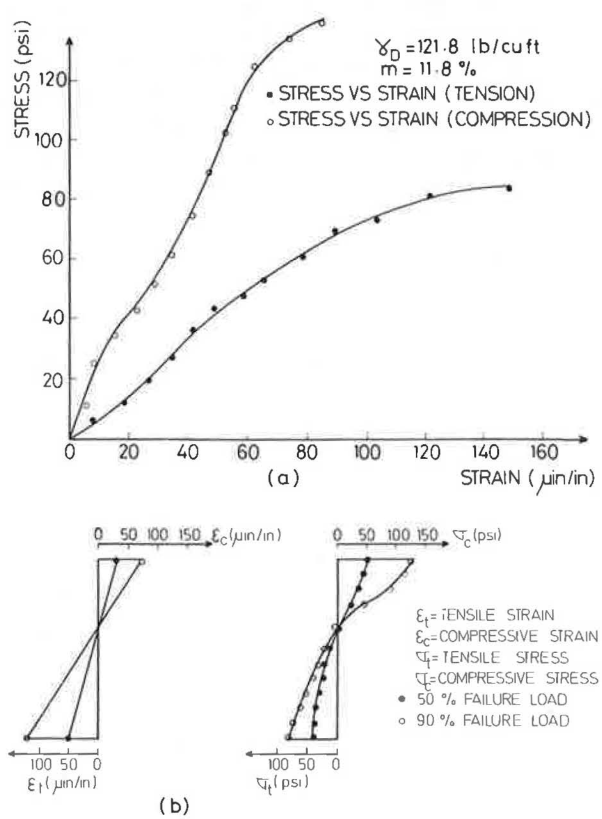

FIGURE 3 Stress-strain behavior of cement-treated sand mix in tension and compression.

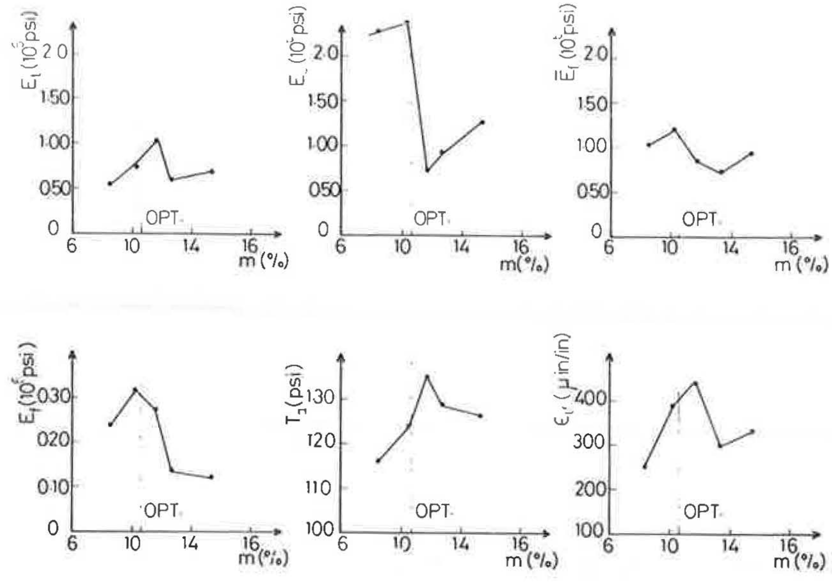

FIGURE 4 Influence of compaction variable on properties of cement-treated silty clay in flexure.

ular ratio (i.e., ratio of compressive modulus, E_c, to tensile modulus, E_t) could be less than or greater than unity depending on compaction moisture content. The modulus in flexure E_f based on deflection measurements at the center of the beam is smaller than the flexural modulus $\overline{E}_f$ associated with moment curvature relations.

3. The influence of increasing dry density γ_D for a given moisture content on the tensile and compressive properties of the cement-treated silty clay and the cement-treated sand mix is shown in Figures 6–9. The tensile modulus, E_t; compressive modulus, E_c; tensile strength, T_a; and tensile strain at failure, ε_{tf}, are normalized by their respective values, E_{to}, E_{co}, T_{ao}, ε_{tfo}, corresponding to maximum dry density γ_{DO} and optimum moisture content using modified AASHTO compaction energy. Results are compared for compaction dry of optimum (opt − 2%), at optimum (opt), and wet of optimum (opt + 2%). Increasing the dry density could yield larger or smaller values of tensile properties than those associated with compaction at maximum dry density and optimum moisture content. In the case of cement-treated silty clay, compaction wet of optimum results in larger values of tensile properties (E_t, T_a, ε_{tf}) than those obtained at optimum or dry of optimum (Figures 6 and 7), whereas lower values of E_t, T_a, and ε_{tf} are observed in the case of the cement-treated sand mix (Figures 8 and 9). The cement-treated silty clay exhibits more shrinkage than

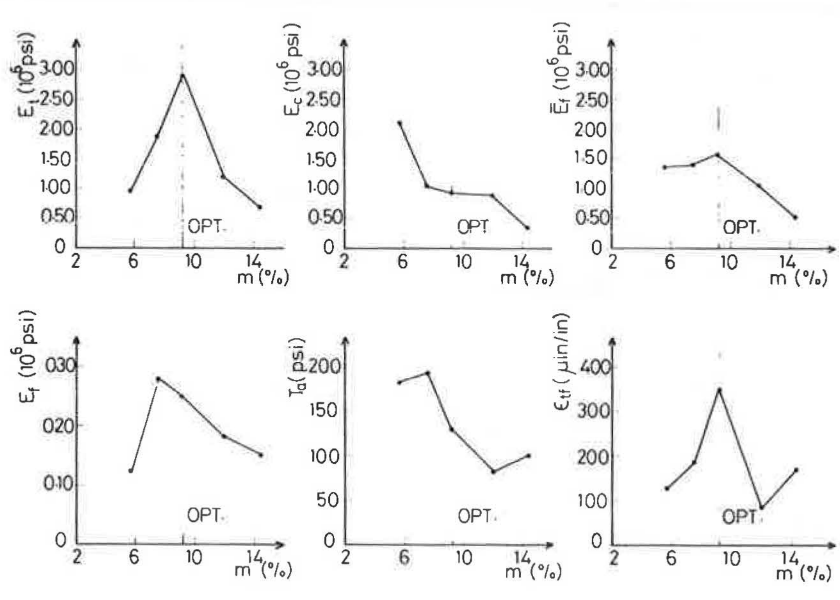

FIGURE 5 Influence of compaction variables on properties of cement-treated sand mix in flexure.

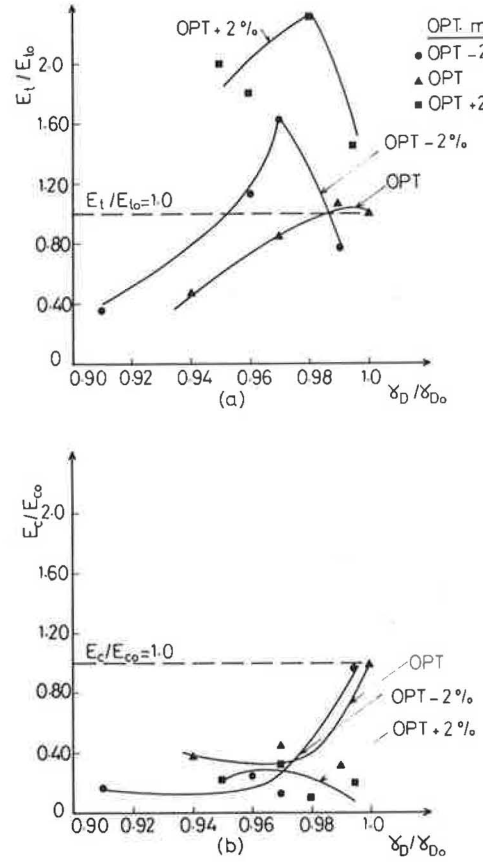

FIGURE 6 Variation of E_c and E_t with γ_D for cement-treated silty clay.

the cement-treated sand mix, which could be reflected as small microcracks in the matrix of the stabilized soil. Compaction wet of optimum in this case could lead to better moisture distribution and cement hydration with the net effect of improving tensile properties.

4. Flexural moduli E_f and $\bar{E}_f$ are generally used to characterize stabilized soils in flexure (*3, 7*). E_f is obtained from central beam deflections, whereas $\bar{E}_f$ is determined by using average top and bottom strains in the flexure test. In both cases, simple beam theory is used without consideration of potential differences in the tensile and compressive stress-strain properties of the stabilized material. Comparisons of tensile modulus E_t with E_f and $\bar{E}_f$ are given in Figure 10. Results indicate that E_t varies in the range of $0.60\bar{E}_f$ and $1.30\bar{E}_f$ with an average close to $\bar{E}_f$ but is much greater than E_f and ranges between $2.6E_f$ and $11.5E_f$. The lower values of E_f are associated with relatively larger central deflections that are probably caused by stress concentrations at the roller supports across both ends of the tested specimen, shear deformations, bimodular material behavior, and an effectively larger specimen in flexure as compared with the zone at which tensile strains are measured. A limited number of observations indicated that deflections at roller supports could reach 27 percent of the total measured central deflection. Correcting E_f for shear deformation effects (*3*) and stress concentrations at roller supports resulted on the average in values that were about 46 percent higher. Even after the corrections had been made, values of E_f were still much lower than those for E_t. It follows that the use of E_f in the design and analysis of stabilized layers should be treated with discretion. On the other hand, $\bar{E}_f$ could be used as an average value for tensile modulus E_t or in conjunction with improved analytical procedures as summarized elsewhere (*2*).

5. Correlation between the flexural strength T_f and the tensile strength T_a for all flexure test data indicates that T_f is in the range of T_a and $1.6T_a$ with a best fit representation of $T_f = 1.15T_a$. The flexural strength, T_f, varies from 70 to 220 psi for the cement-treated silty clay and from 30 to 320 psi for the cement-treated sand mix.

6. The tensile strain on the underside of cement-treated layers has been proposed by many investigators (*6*) as an alternative criterion to the tensile stress for design purposes. However, most available data for tensile strains are determined from flexural tests as the ratio of flexural stress to flexural modulus, E_f, and not as a direct measurement of strains on the underside of beam specimens. Results of this study indicate that measured tensile strain values at failure, ε_{tf}, vary from 200 to 600 μin./in. for the cement-treated silty clay and from 70 to 300 μin./in. for the cement-treated sand mix. An attempt to correlate ε_{tf} with corresponding values of T_f reflected a considerable scatter in the data (i.e., a relatively small coefficient of determina-

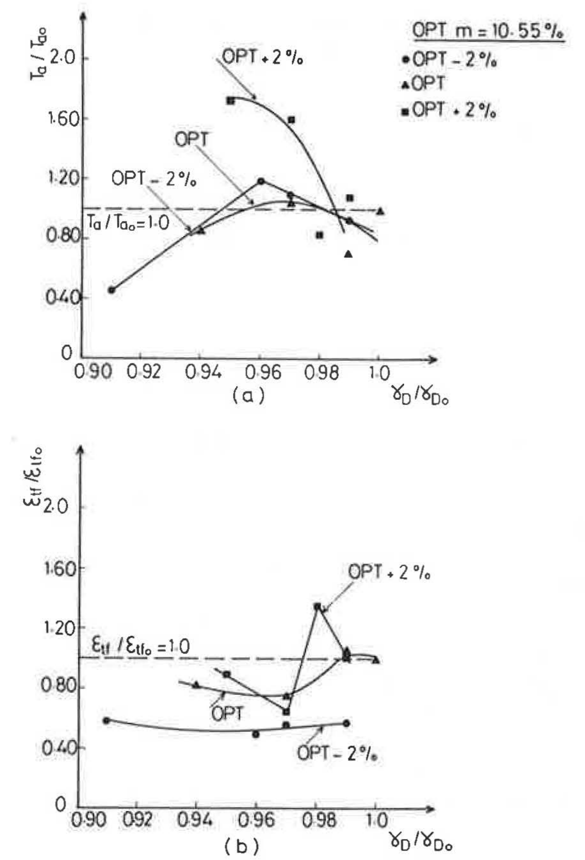

FIGURE 7 Variation of T_a and ε_{tf} with γ_D for cement-treated silty clay.

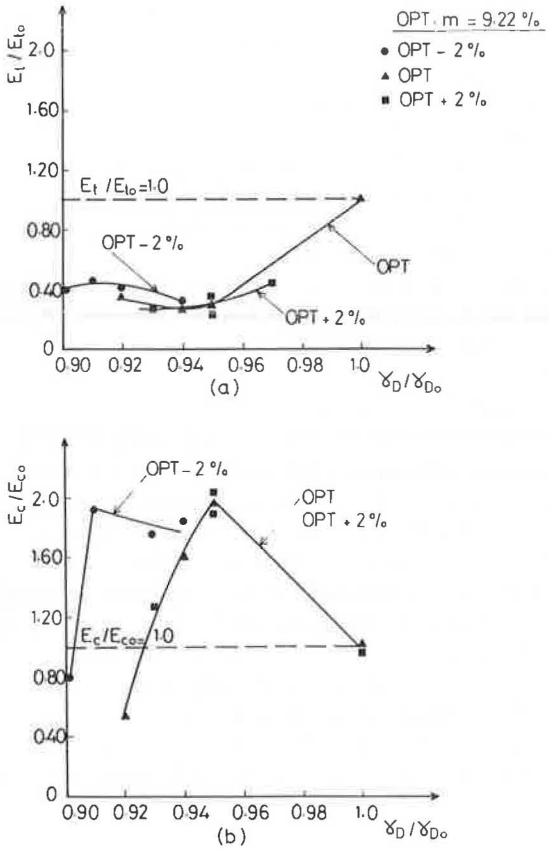

FIGURE 8 Variation of E_c and E_t with γ_D for cement-treated sand mix.

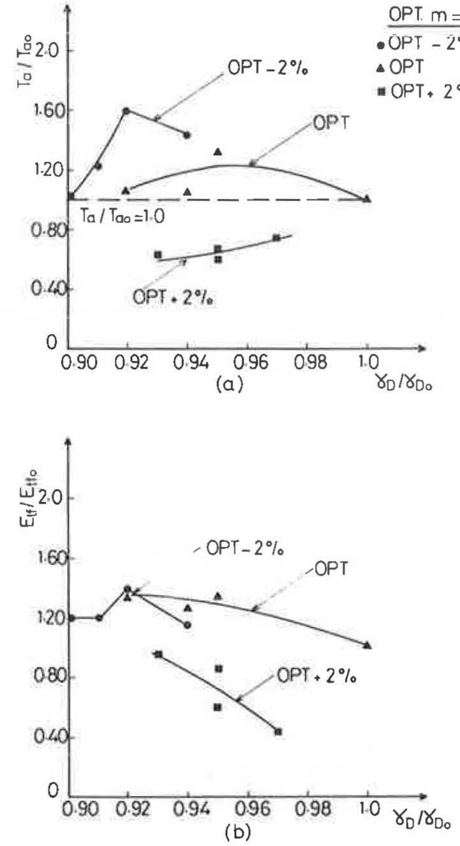

FIGURE 9 Variation of T_a and ε_{tf} with γ_D for cement-treated sand mix.

tion, R^2) The following relations, however, demonstrate the trend of variation.

For the cement-treated silty clay,

$$\varepsilon_{tf} = 423 - 0.61T_f \qquad (R^2 = 0.58) \tag{8}$$

and for the cement-treated sand mix,

$$\varepsilon_{tf} = 405 - 0.96T_f \qquad (R^2 = 0.26) \tag{9}$$

where ε_{tf} is expressed in microinches per inch and T_f is in pounds per square inch.

7. The influence of compaction variables, stress level, curing age, and cement content on bimodular ratio E_c/E_t is shown in Figures 11–15. Figures 11 and 12 are contour plots of E_c/E_t for the cement-treated silty clay and the cement-treated sand mix in terms of compaction moisture content and dry density. In the case of the cement-treated silty clay, an increase in compaction moisture content for a given dry density will result in a decrease in E_c/E_t followed by an increase for moisture content values wet of optimum (Figure 11). An opposite trend is observed for the cement-treated sand mix, in which E_c/E_t increases with compaction moisture content followed by a decrease for compaction wet of optimum (Figure 12). The variation of E_c/E_t with applied stress level (i.e., ratio of applied load to rupture load) is shown in Figure 13. Results indicate that the bimodular ratio is stress dependent and tends to increase in general for stress levels greater than 80 percent. The influence of curing age and cement content using test groups C_5,S_5 and C_6,S_6, respectively, is presented in Figures 14 and 15. Results of the limited number of tests

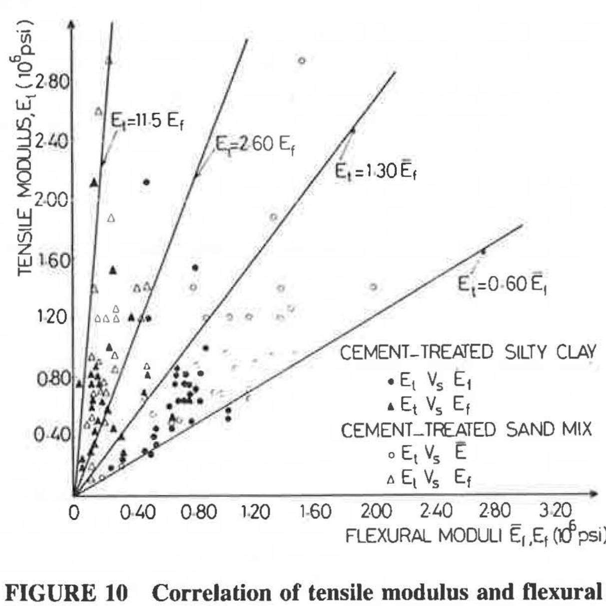

FIGURE 10 Correlation of tensile modulus and flexural moduli.

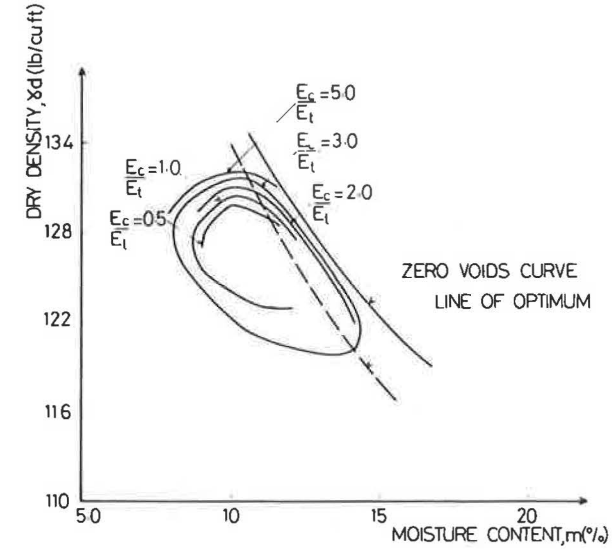

FIGURE 11 Influence of compaction variables on bimodular ratio for cement-treated silty clay.

performed reflect in general a decreasing tendency of bimodular ratio with increasing cement content and curing age. Correlations of compressive modulus, E_c; tensile modulus, E_t; and bimodular ratio, E_c/E_t, with flexural strength, T_f, are shown below. Although E_c and E_t tend to increase with increasing T_f, E_c/E_t would decrease in general. Moreover, lower values of E_c and E_t and higher values of E_c/E_t are obtained for a given T_f in the case of the cement-treated silty clay in comparison with the cement-treated sand mix.

For the cement-treated silty clay,

$$E_c = 66.9 + 5.39T_f \qquad (R^2 = 0.44) \qquad (10)$$

$$E_t = -35.9 + 5.07T_f \qquad (R^2 = 0.63) \qquad (11)$$

$$E_c/E_t = 5.43 - 0.02T_f \qquad (R^2 = 0.23) \qquad (12)$$

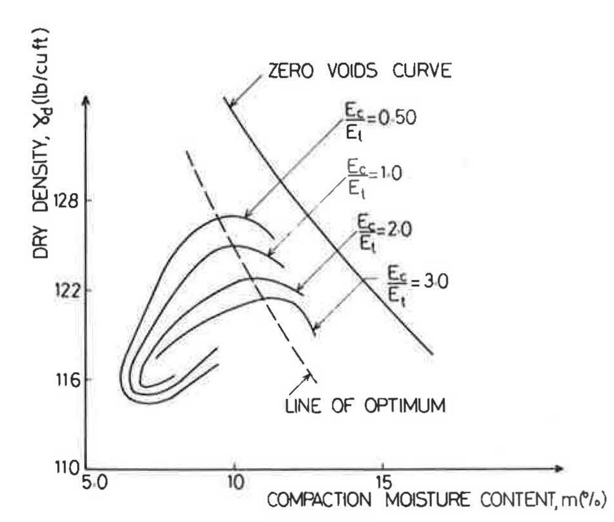

FIGURE 12 Influence of compaction variables on bimodular ratio for cement-treated sand mix.

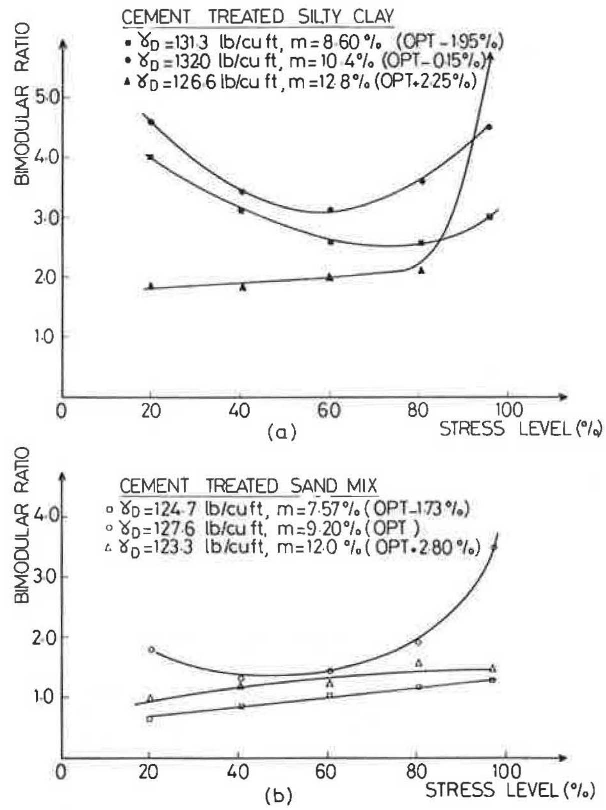

FIGURE 13 Influence of stress level on bimodular ratio.

and for the cement-treated sand mix,

$$E_c = 320 + 7.84T_f \qquad (R^2 = 0.43) \qquad (13)$$

$$E_t = -108 + 9.94T_f \qquad (R^2 = 0.68) \qquad (14)$$

$$E_c/E_t = 3.31 - 0.01T_f \qquad (R^2 = 0.24) \qquad (15)$$

where E_c and E_t are expressed in kips per square inch and T_f is in pounds per square inch.

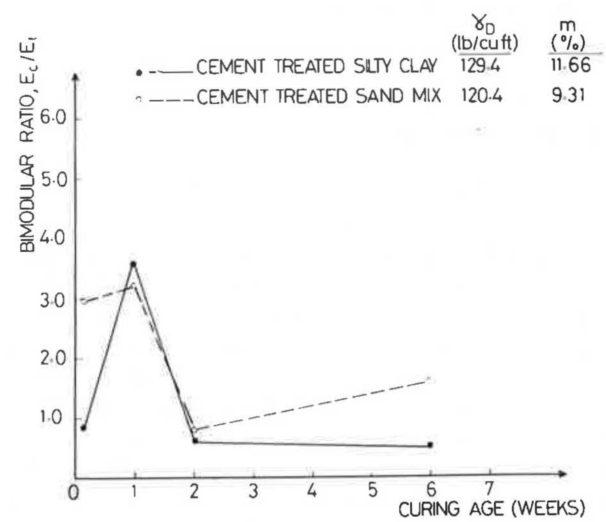

FIGURE 14 Influence of curing age on bimodular ratio.

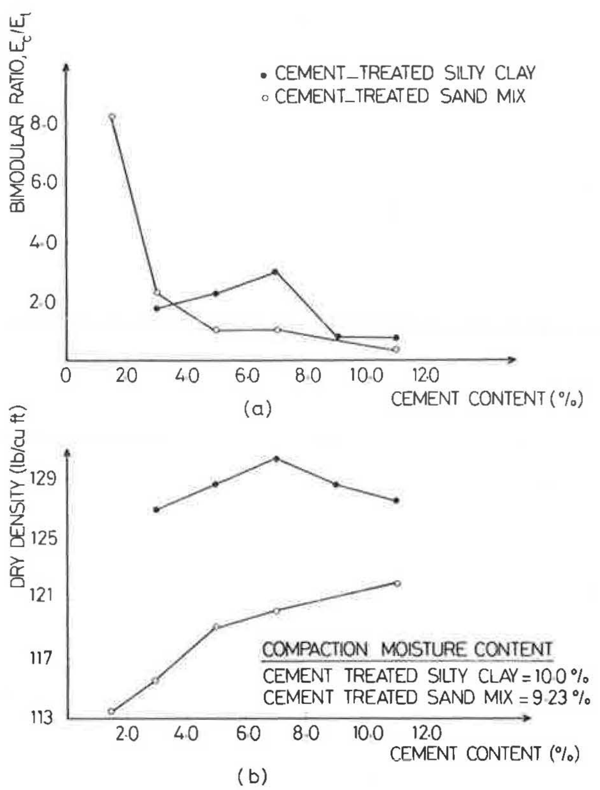

FIGURE 15 Influence of cement content on bimodular ratio.

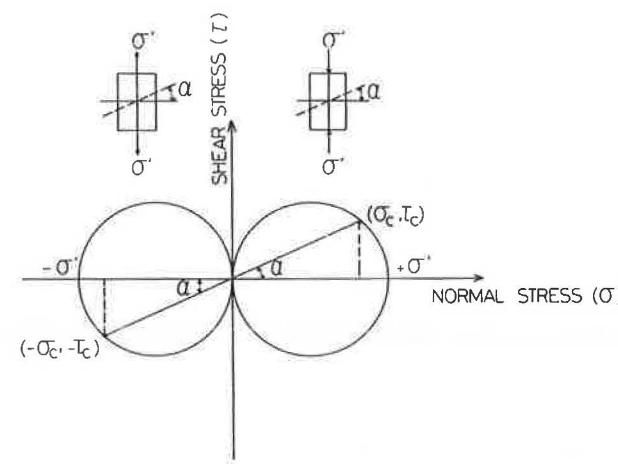

FIGURE 16 Stress state on a given plane in specimens under direct tension and compression.

MECHANISMS OF BIMODULAR BEHAVIOR

Flexural beam test results indicate that for the cement-treated silty clay the bimodular ratio is in the range of 0.5 to 5, whereas for the cement-treated sand mix it ranges from 0.5 to 3. Similar behavior is observed for cement-treated materials under direct tension and compression testing, in which bimodular ratio values ranging from 1 to 10 have been reported (*8, 9*). The probable mechanisms of bimodular behavior could be described as one or more of those discussed in the following sections.

Resistance to Shear under Normal Tensile and Compressive Stresses

It is assumed that under normal tensile and compressive stresses, the stabilized soil will exhibit a greater resistance to shear deformation along a given plane if the applied normal stress on that plane is compressive than if the same applied stress is tensile. Schematically this is shown using a Mohr circle representation for a uniaxial tensile and compressive stress application (Figure 16). On a given plane, the normal stress is compressive under uniaxial compression, whereas it is tensile under uniaxial tension. The magnitude of the shear stress acting on the same plane is equal in both cases, indicating a greater shear deformation potential under uniaxial tension than under uniaxial compression. This would result in a greater modulus in compression than in tension for the same applied uniaxial stress.

Fracture Propagation of Flaws and Microcracks

Fracture mechanics principles are used to demonstrate the effect of cracking on the stress-strain behavior. For a given specimen with a thin microcrack of length $2a$, as shown in Figure 17, the propagation of the crack under a given tensile stress associated with applied displacement (Δ) or

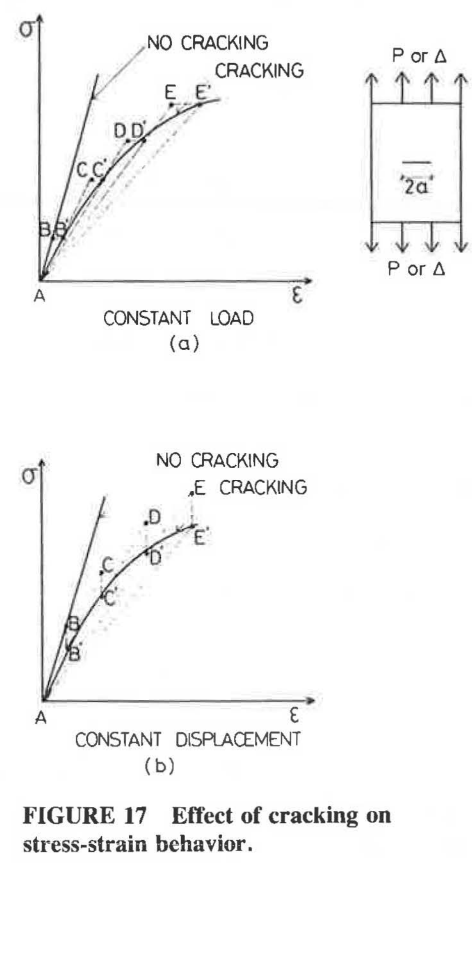

FIGURE 17 Effect of cracking on stress-strain behavior.

tensile load (P) would result in a release of stored elastic energy at a constant stress (Figure 17a) or at a constant strain (Figure 17b), thereby yielding the stress-strain representation (A,B',C',D').

Local Stiffness Variation Within the Material

The material in this case is discretized into elements (i,j,k) as shown in Figure 18. Assuming that each element has a designated stiffness E_{ijk}, the measured modulus E under uniaxial tension will be given by

$$E = 1/C \qquad (16)$$

where

$$C = \frac{ml}{n}\left(\frac{1}{\sum_{i=1}^{1}\sum_{j=1}^{m} E_{ijl} + \ldots + \sum_{i=1}^{1}\sum_{j=1}^{m} E_{ijn}}\right) \qquad (17)$$

such that

l = number of elements in the i-direction,
m = number of elements in the j-direction, and
n = number of elements in the k-direction.

A loss of element stiffness under uniaxial tensile stress could be induced by an existing microcrack or by crack propagation at the tip of a flaw or a discontinuity. As a result, C will increase and the measured modulus E will decrease. Because stabilized materials are weaker in tension than in compression (*8, 10*), it is more likely that loss of element stiffness will occur if the applied stress is tensile than if it is compressive. The measured compressive modulus is therefore expected to be larger than the measured tensile modulus for the same applied uniaxial stress. With this discretized model it could also be inferred that the probability of encountering an element with low stiffness increases with increasing specimen volume V as shown in Figure 18. The effect of size on measured stiffness will be more significant under tensile stresses than under compressive stresses. Mathematical treatment by other investigators (*11*) yielded similar results concerning the effect of specimen size on the probability of failure of brittle solids.

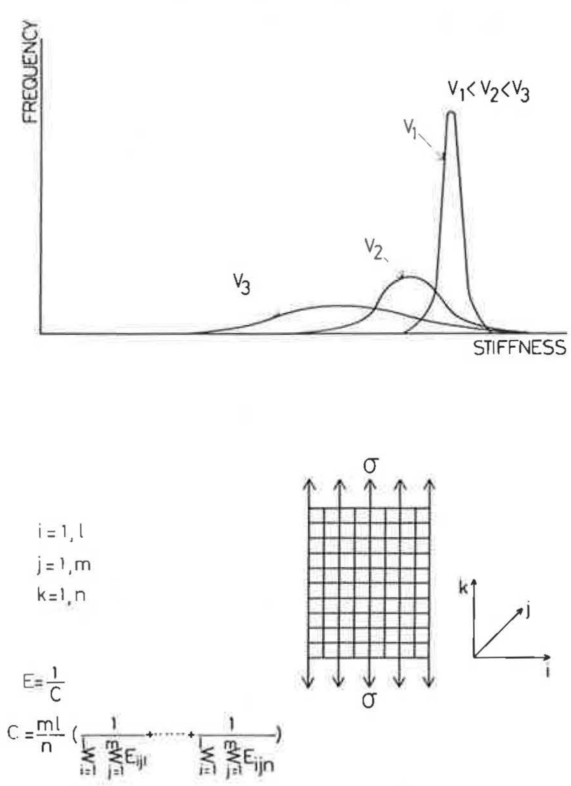

FIGURE 18 Discrete model and probable effect of specimen size on stiffness.

SIGNIFICANCE OF BIMODULAR BEHAVIOR

A two-layer pavement system consisting of a cement-treated base over a subgrade was analyzed to study the influence of bimodular properties on response and fracture behavior under repeated traffic loads. An iterative technique utilizing the finite-element method and a fatigue failure model for the cement-treated layer was employed. Plane strain conditions were assumed. Details of the analytical procedure have been presented elsewhere (*12*). A finite-element representation of the pavement system is shown in Figure 19.

Results of the analysis indicate that structural response is significantly influenced by the bimodular properties of the cement-treated base (Figure 20). A reduction in tensile modulus, for example, from a value equal to its compressive modulus (i.e., bimodular ratio of 1) to a value equal to one-tenth the compressive modulus (i.e., bimodular ratio of 10) results in an increase in subgrade vertical stress, σ_v, and surface deflection, d. However, the most significant influence seems to be associated with the tensile stress σ_t

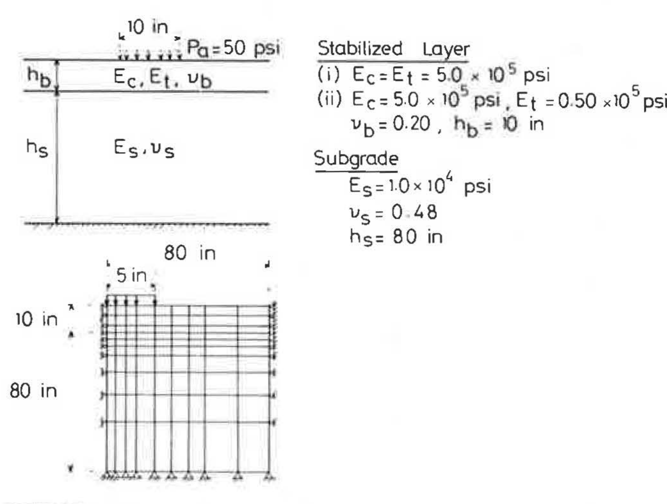

FIGURE 19 Finite-element representation of pavement section.

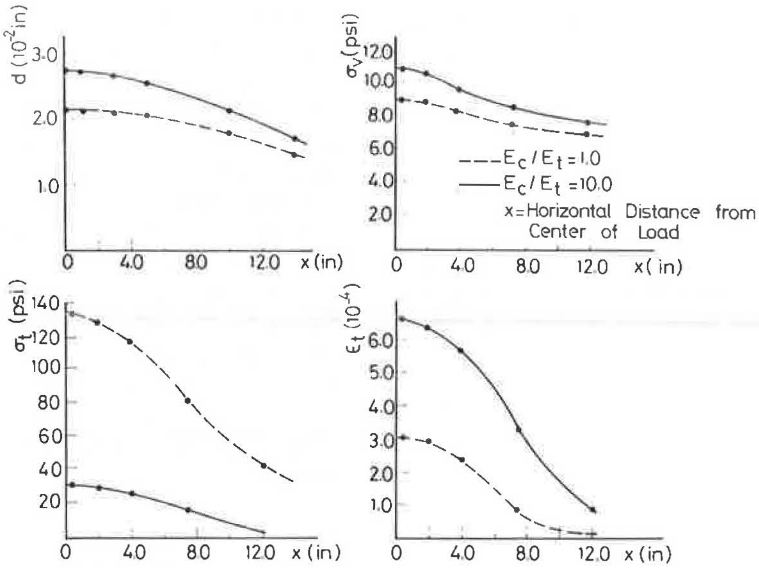

FIGURE 20 Response of stabilized layer under applied load.

and the tensile strain ε_t on the underside of the base. The maximum tensile stress is reduced about 5 times, whereas the maximum tensile strain becomes twice as much.

The influence of the bimodular ratio on fatigue crack initiation and propagation for a given number of load repetitions (106 repetitions in this case) is shown in Figure 21. For a given thickness of base, flexural strength, and compressive modulus, a decrease in bimodular ratio seems to increase the resistance of the stabilized layer to fatigue crack initiation and propagation. Moreover, a smaller increment of load is required to propagate the crack from the underside of the base to its surface for the case of $E_c/E_t = 10$ as compared with the case of $E_c/E_t = 1$, indicating a higher rate of crack propagation.

Similar analyses were also conducted to investigate the fatigue behavior of the stabilized base when the cement-treated silty clay was used as compared with use of the cement-treated sand mix. The two-layer representation of the pavement section is shown in Figure 19. The applied load needed for crack initiation and propagation was estimated for different values of flexural strength and tensile and compressive moduli as determined from Equations 10–15. Results are presented in Figure 22. Increasing the flexural strength would increase the load required for fatigue crack initiation on the underside of the base and propagation to its surface. The increase in flexural strength in

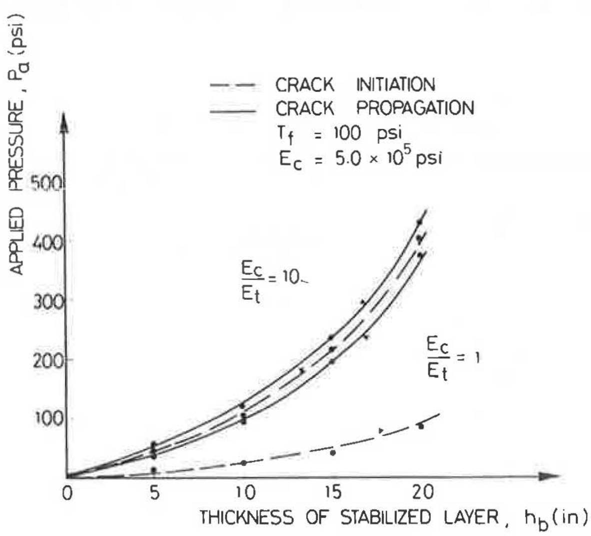

FIGURE 21 Influence of bimodular properties on fatigue crack initiation and propagation after 10^6 repetitions.

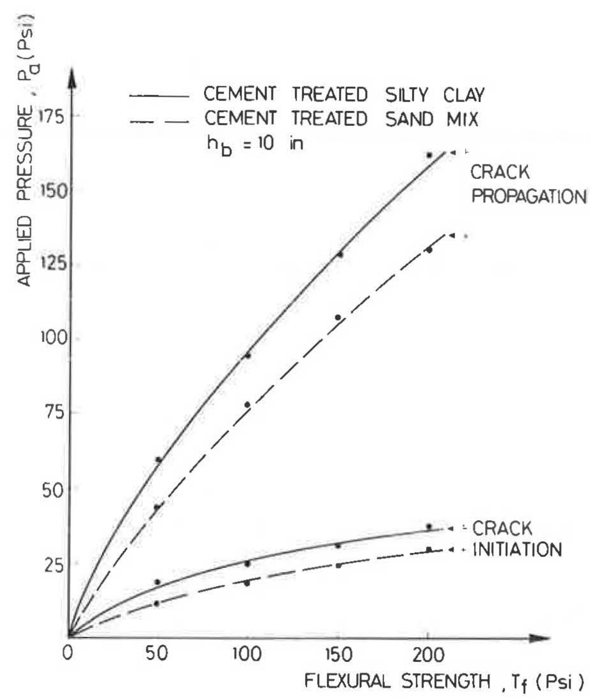

FIGURE 22 Fatigue behavior after 10^6 repetitions: 10-in. base of cement-treated silty clay versus cement-treated sand mix.

this case seems to outweigh the reduction in fatigue load capacity associated with the resulting higher compressive modulus and lower bimodular ratio, with the net effect of enhancing the fatigue resistance of the base. Moreover, for a given flexural strength, the cement-treated silty clay seems to exhibit more resistance to fatigue loading when used as a base in comparison with the cement-treated sand mix.

These results agree with similar conclusions presented by Williams (*13*). They are, however, tentative. Additional research is needed to compare tensile and compressive properties of stabilized soils using static and repeated load tests. Of particular interest is the influence of fatigue on bimodular behavior. Fatigue data for a cement-treated clayey gravel presented by Pretorius (*14*, p. 67) show an increase in bimodular ratio from an initial value of 1.2 to about 4 during flexure fatigue testing.

SUMMARY AND CONCLUSIONS

Flexure tests have been used to study the flexural behavior of a cement-treated silty clay and a cement-treated sand mix. The influence of compaction variables, cement content, and curing age on stress-strain characteristics in tension and compression, flexural strength, tensile strength, tensile strain at failure, and flexural moduli have been investigated.

The flexural modulus $\bar{E}_f$ determined from moment curvature relations has been found to attain an average value essentially equal to the tensile modulus E_t, whereas the flexural modulus E_f obtained using simple beam theory and central beam deflection is much smaller than E_t. Although $\bar{E}_f$ could be used as an average estimate for tensile modulus E_t and in conjunction with improved analytical procedures as summarized elsewhere (*2*), the use of E_f in design and analysis of stabilized layers should be treated with discretion.

Computation of flexural strength T_f using simple beam theory assumptions yields values that are essentially equal to 1.15 times the actual tensile strength T_a associated with tensile failure on the underside of the beam. The tensile strain at failure, ε_{tcf}, varies from 200 to 600 μin./in. for the cement-treated silty clay and from 70 to 300 μin./in. for the cement-treated sand mix. An increase in flexural strength T_f results in a reduction of failure tensile strain ε_{tf}.

Stress-strain predictions using top and bottom strain measurements in beam specimens indicate different load-deformation properties in tension and compression. Values of compressive modulus E_c, tensile modulus E_t, tensile strength T_a, and tensile strain at failure ε_{tf} could be higher or lower than the corresponding values at optimum moisture content and maximum AASHTO dry density, depending on type of stabilized soil, compaction moisture content, and dry density. The bimodular ratio E_c/E_t ranges between 0.5 and 5 for the cement-treated silty clay and from 0.5 to 3 for the cement-treated sand mix. Although E_c and E_t tend to increase with increasing T_f, E_c/E_t would decrease in general. The observed differences in compressive and tensile moduli have been explained using a number of mechanistic models.

Results of the analysis indicate that the bimodular properties have a significant effect on the traffic-induced stresses and strains on the underside of the stabilized base and on its fracture behavior in terms of fatigue crack initiation and propagation. The proper assessment of these properties is therefore desirable for developing a better understanding of the behavior of stabilized layers under applied traffic loads.

ACKNOWLEDGMENTS

This work was supported by a grant from the University Research Board of the American University of Beirut. Laboratory assistance by H. Minassian, S. Saboudjian, B. Zeid, and M. Itani is gratefully acknowledged.

REFERENCES

1. L. Raad, C. L. Monismith, and J. K. Mitchell. Crack Propagation in Soil-Cement Bases Subjected to Repeated Wheel Loads. In *Transportation Research Record 690*, TRB, National Research Council, Washington, D.C., 1978, pp. 1–5.
2. L. Raad. Behavior of Stabilized Layers Under Repeated Loads. In *Transportation Research Record 1022*, TRB, National Research Council, Washington, D.C., 1985, pp. 72–79.
3. E. J. Felt and M. S. Abrams. Strength and Elastic Properties of Compacted Soil-Cement Mixtures. In *Special Technical Publication 206*, American Society for Testing and Materials, Philadelphia, Pa., Sept. 1956, pp. 153–173.
4. J. S. Gregg. The Significance of Compressive, Tensile, and Flexural Strength Tests in the Design of Cement-Stabilized Pavement Foundations. In *Proceedings, Fourth Regional Conference for Africa on Soil Mechanics and Foundation Engineering*, Capetown, South Africa, Dec. 1967, pp. 185–190.
5. J. L. M. Scott. *Flexural Stress-Strain Characteristics of Saskatchewan Soil-Cements*. Technical Report 23. Saskatchewan Department of Highways and Transportation, Regina, Saskatchewan, Canada, Dec. 1974.
6. E. Otte, P. F. Savage, and C. L. Monismith. Structural Design of Cement-Treated Layers. *Journal of the Transportation Engineering Division*, ASCE, Vol. 108, No. TE4, July 1982, pp. 428–446.
7. L. P. Sudath and M. R. Thompson. *Load-Deflection Behavior of Lime Stabilized Layers*. Technical Report M-118. Construction Engineering Research Laboratory, Urbana-Champaign, Ill., Jan. 1975.
8. L. Raad, C. L. Monismith, and J. K. Mitchell. Tensile Strength Determinations of Cement-Treated Materials. In *Transportation Research Record 641*, TRB, National Research Council, Washington, D.C., 1977, pp. 48–51.
9. H.E. Bofinger. *The Measurement of the Tensile Properties of Soil-Cement*. Report LR365. U.K. Transport and Road Research Laboratory, Crowthorne, Berkshire, England, 1970.
10. A. A. Griffith. Theory of Rupture. In *Proceedings of First International Congress for Applied Mechanics*, Delft, Netherlands, 1924, pp. 55–63.
11. H. L. Oh and I. Finnie. On the Location of Fracture in Brittle Solids. I: Due to Static Loading. *International Journal of Fracture Mechanics*, Vol. 6, 1970, pp. 287–300.

12. L. Raad, C. L. Monismith, and J. K. Mitchell. Crack Propagation in Soil-Cement Bases Subjected to Repeated Wheel Loads. In *Transportation Research Record 690*, TRB, National Research Council, Washington, D.C., 1978, pp. 1–5.
13. R. I. T. Williams. Properties of Cement-Stabilized Materials. *Journal of the Institution of Highway Engineers*, Feb. 1972, pp. 5–19.
14. P.C. Pretorius. Design Considerations for Pavements Containing Soil-Cement Bases. Ph.D. dissertation. University of California, Berkeley, 1970.

Publication of this paper sponsored by Committee on Soil-Portland Cement Stabilization.